# Atomic Scale Investigation

# of

# Tin Selenide

**A thesis submitted towards partial fulfilment of**

**BS-MS Dual Degree Programme**


**By**

**Thasneem A**

**(BS-MS student, Registration No. : 20121067)**

**Under the guidance of**

**Dr. Aparna Deshpande**

**Department of Physics**

**Indian Institute of Science Education and Research (IISER) Pune, India**

## Certificate

This is to certify that this dissertation entitled "**Atomic scale investigation of tin selenide**" towards the partial fulfillment of the BS-MS dual degree programme at the Indian Institute of Science Education and Research Pune, represents original research carried out by **Thasneem A.** at IISER Pune under the supervision of "**Dr.Aparna Deshpande**, Assistant Professor, Department of Physics, IISER Pune" during the academic year of 2016-2017.

Date: 23/03/2017
Place : Pune:

**Dr.Aparna Deshpande**
Assistant Professor
Department of Physics
IISER Pune

## Declaration by the candidate

I hereby declare that the matter embodied in the report entitled "**Atomic scale investigation of Tin Selenide**" are the results of investigation carried out by me at the department of physics, IISER Pune, Under the supervision of Dr. Aparna Deshpande and the same has not been submitted elsewhere for any other degree.

Thasneem A

Date: 22-03-2017

Place: Pune

# Acknowledgements

I would like to thank my guide Dr Aparna Deshpande for giving me an opportunity to work on this project using Ultra High Vacuum Low Temperature Scanning Tunnelling Microscopy (UHV LT STM). Without her suggestions, guidance and motivation given at every stage of the project, I would not have finished this project successfully. I specifically thank Dr Luminita Harnagea for giving me the synthesized SnSe, Scanning Electron Microscopy and X ray diffraction data and for all discussions regarding SnSe. I thank my lab mates for making our lab environment nice to work with. I specifically express my sincere gratitude to Rejaul bhayya for all his advices and inputs for my project. I am grateful to Imran bhayya for all doubt clearing sessions and Navathej for supporting me. I also thank Sumati madam and Sadhu sir for giving me valuable suggestions for my project. Special thanks to Nilesh sir and Prashant sir for lending all technical supports. I would like to express my heartfelt gratitude to the Department of Physics, IISER Pune for all the facilities provided. I thank Nithin, Surya, Anagha, Akhil, Kavya and Anjana for making my life easier in IISER. Last but not the least, I thank my dear family for supporting me during my good and bad times.

## TABLE OF CONTENTS

# List of Abbreviations

UHV – Ultra High Vacuum

LT – Low Temperature

STM- Scanning Tunnelling Microscope

FESEM – Field Emission Scanning Electron Microscope

XRD – X ray Diffraction

AFM- Atomic Force Microscope

HRTEM – High Resolution Transmission Electron Microscope

SAD- Selected Area Diffraction

MBE- Molecular Beam Epitaxy

ARPES – Angle Resolved Photo Emission Spectroscopy

# Abstract

SnSe is a p type semiconductor belonging to IV-VI group of chalcogenides. It is a layered material with strong in plane covalent interaction and weak inter layer Van der Waal's interaction. SnSe in Cmcm phase is known for its highest figure of merit (ZT) value of 2.6 at 923K. This behaviour is attributed to its ultra-low thermal conductivity of around 0.24 W/mK. Even though few studies on surface properties of SnSe are reported, the local electronic property of the sample is not investigated thoroughly. In this work, Scanning Tunnelling Microscopy and Scanning Tunnelling Spectroscopy studies were carried out to understand the local electronic properties of the SnSe at 77K and at 300K. SnSe was synthesized using chemical vapour transport technique and studies were performed on Pnma phase of the crystal. Investigation of intrinsic defects on the single crystal was performed in Ultra High Vacuum Low Temperature Scanning Tunnelling Microscopy.

# CHAPTER I

# INTRODUCTION

This chapter gives a brief outline about layered materials and thermoelectric materials**.** It is followed by a briefing about tin selenide single crystal (SnSe) and the literature survey of SnSe.

## 1.1 Introduction

Our lives are finely tuned by technologies. Development of technologies lies in the basic science research, like the discovery of X rays by Roentgen. Influence of X rays could be seen in many regimes starting from treatments in hospitals, screening of baggage at airports, to research labs like x-ray diffraction. As technologies are improving with time, the need for energy is also increasing. So energy conversion and energy storage in the most efficient way is a question of importance now. Usage of non-renewable sources like fossil fuels will not only deplete the source but cause pollution also. Increase in carbon dioxide in the atmosphere leads to global warming and thus affects the equilibrium of nature. For the last few decades studies have turned to focus on renewable sources like solar energy, wind energy, hydro energy and geothermal energy. However there is always quite a significant amount of energy loss in these processes. People realise the importance of harvesting such an energy loss by using thermo electric materials, piezo electric materials, pyro electric materials and so on [1,2].Focus is given on materials which could be used to increase the efficiency in this field.

Nano materials enhance the efficiency in applications due to their high surface to volume ratio, change in physical and chemical properties, tuneable band gap and so on. Materials can be broadly classified into zero dimensional (0 D), one dimensional(1 D),two dimensional(2 D) and three dimensional(3 D) depending on its electron movements. For a 0D material like quantum dot the electrons are confined in all 3 dimensions and 1D material like nanotubes electrons are confined in one dimension. Then there are two dimensional materials (2D) like graphene which are atomically thin and having confined electronic movement in one plane. Graphene is the first 2D material discovered by Andre Geim and Novoselov which earned them a Nobel prize in Physics in 2010. It is followed by hexagonal boron nitride, Molybdenum disulphide, Black Phosphorus, to name a few.

Tuning the properties of materials and discovering new materials paves the way for making applications better. Investigating the bulk and surface properties of materials plays a crucial role in understanding a material thoroughly. The field of condensed matter physics and material science works hand in hand to produce significant results.

## 1.2 Layered Materials

”Layered Materials “are a class of two dimensional (2D) materials which possess strong in plane covalent interaction and weak inter layer Van der Waal’s interaction. Since the bonds

between the neighbouring layers are not strong, it is possible to exfoliate the crystal from bulk to atomically thin layers. Most of the monolayers of layered materials are stable in the ambient conditions and thus capable for device applications [3]. 2D materials show exceptional electronic and optical properties due to the confinement of electrons in one plane. Graphene, a 2D sheet of carbon atoms is a layered material. Graphene is known for its exceptional properties. To name a few, it has very high mobility of the order of $10^{(5)}$ $cm^2$/ Vm at ambient conditions, shows metallic behaviour, and ballistic transport. The electrons in graphene are described using Dirac equation since the carriers move like relativistic particles [ 4]. Transition Metal Dichalcogenides, are represented by $MX_2$ where M is a transition metal and X is a chalcogen(X = S, Se, Te) and Transition Metal Oxides like $MoO_3$, $WO_3$, $TiO_2$ broadened the field of 2D materials [3]. Narrowing down to fewer layers produces a remarkable change in their behaviour chemically, optically, electronically. Fewer layers have a substantial increase in its surface area compared to that of Bulk. This could change its chemical and physical properties compared to that of bulk. Materials like Molybdenum disulphide show a transition from indirect to direct bandgap as we go from bulk to monolayer. Direct bandgap is more favourable for device applications compared to indirect bandgap due to its less energy loss. Similarly, few layers of other 2D materials also shows remarkable properties which is quite interesting. For producing fewer layers from bulk, techniques like micro mechanical cleavage, liquid exfoliation, heating, could be used. [5].

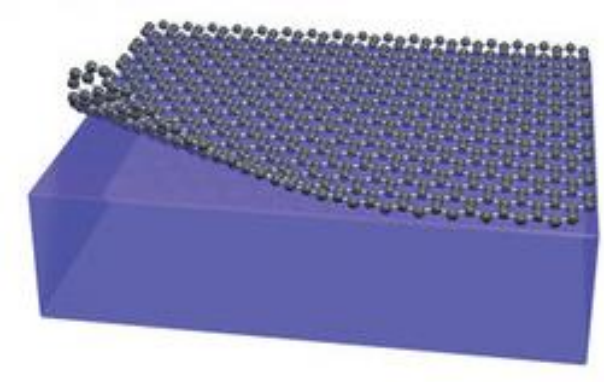

**Figure 1.1 shows an illustration of a 2D sheet that can be exfoliated from a layered material**.

## 1.3 Thermoelectric materials

Materials which can convert heat energy into electrical energy and electrical energy into heat energy are termed as thermoelectric materials. Two types of thermoelectricity are Seebeck effect and Peltier effect. In Seebeck effect, a temperature gradient (ΔT) is applied to a junction of different materials. Corresponding change in voltage (ΔV) is measured across the junction.

Seebeck coefficient, S is given by ΔV/ΔT

In Peltier effect, a potential difference is applied to a junction of different materials and variation in temperature is measured in the junction. Peltier coefficient of a material is defined as the ratio of amount of heat carried per unit charge.

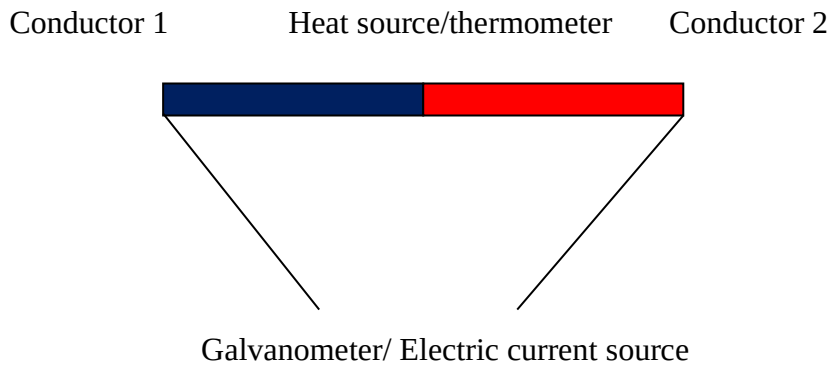


**Figure 1.2: Schematic diagram showing Seebeck effect and Peltier effect.** Heat source which is connected to the junction of two different conductors causes a flow of current through them. This is measured using a Galvanometer. Similarly, current passed through these conductors would produce a potential difference and it is measured using thermometer (Adapted from [7]).

**Figure of merit (ZT):** ZT is a dimensionless quantity which explains the thermoelectric efficiency of materials.

$$ZT = S^2 б\ T/\kappa$$

Where S is the Seebeck coefficient, б is the electronic conductivity, T is the temperature and κ is the combined thermal conductivity of phonons and electrons.

Materials like SnSe, $Bi_2Se_3$, $Bi_2Te_3$, Sb doped ZnO , Bi doped SnSe are few examples of thermoelectric materials. SnSe has got a wide attention in recent years due to its high ZT value

of 2.6 in Cmcm phase at a temperature of 923K. This is attributed to its ultralow thermal conductivity value.

### 1.4 Tin Selenide

Tin Selenide (SnSe) is a p type semiconductor belonging to IV-VI group chalcogenides. It is a layered material with strong covalent interaction between Sn and Se in plane and weak inter layer Van der Waal's interaction. The unit cell of SnSe has eight atoms in two adjacent layers. Each of the Sn/Se atoms are strongly bonded to three nearest Se/Sn atoms in the same layer. The interlayer distance of SnSe is 0.3465 nm [8].Single layer thickness of SnSe is 0.6nm [9] .Bulk SnSe has an indirect band gap of 0.58 eV and a direct band gap of 0.98 eV. Monolayer SnSe has an indirect band gap of 0.89 eV and a direct band gap of 1.08 eV [10].

SnSe is in orthorhombic Pnma phase at ambient conditions. It shows structural transition from Pnma phase to the more symmetric Cmcm phase either above 750K or from 15.5GPa to 19.3GPa [11,12]. The transition from Pnma to Cmcm is attributed to the dislocation of Sn/Se atoms along (010) direction. Further rise in pressure pushes the Cmcm phase to Fm3m phase. This phase change from Cmcm to Fm3m is due to the additional bonding between Sn and Se atoms upon compression. Upon applying pressure above 50.1GPa, rocksalt phase of SnSe which is in Fm3m phase is experimentally realized. In this stage, SnSe which became compressed into Rocksalt structure shows signs of superconductivity [12].

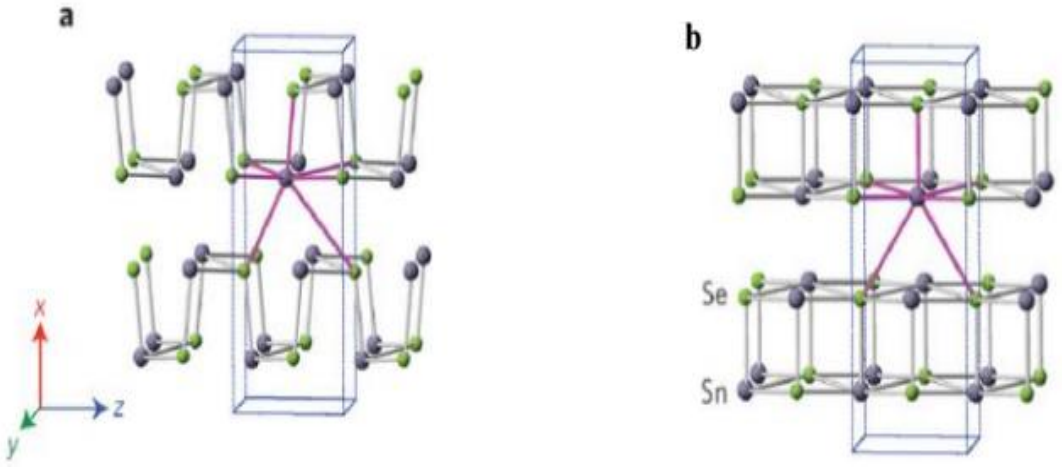


Figure 1.3 (a) shows the orthorhombic Pnma structure of SnSe and (b) shows the more symmetric SnSe in Cmcm phase. The structural transition of SnSe from Pnma to Cmcm could be observed at high pressure and temperature above 780K. [13]

Figure of Merit, ZT shows the ability of a material to generate thermoelectric power efficiently. SnSe in Cmcm phase has the highest reported thermoelectric figure of merit, ZT of 2.6 ± 0.3 at 923K along b direction in Cmcm phase. This is due to the ultra-low thermal conductivity and anisotropical structure of SnSe [14].

Since this behaviour is achieved at quite a high temperature, attempts are made to bring down the temperature. If efficiency could be increased at lower temperature itself, energy wastage could be reduced drastically. This could be achieved by doping SnSe. And if SnSe is doped, carrier concentration could be enhanced and thus the power factor leading to a increment in the ZT value.

The carrier concentration and Seebeck coefficient is increased for n type SnSe doped with $BiCl_3$. This system shows a ZT value of 0.7 at 793K [15]. Instead of a Bi compound, if SnSe is doped with pristine Bismuth, ZT factor goes up to 2.2 at 923K [16]. Polycrystalline p type SnSe, which is doped with Zn ,Na and Ag are capable for giving thermoelectric figure of merit values like 0.96, 0.8 and 0.6 at 873 K , 773K and 750K respectively [17,18,19].

### 1.5 Literature review on Scanning Tunnelling Microscopy studies of SnSe

STM is used to do real space imaging of conducting samples. It is extensively used to visualise the underlying atomic structure, to probe the local density of states of the sample and to do defect investigation. STM is the only non-invasive technique which could be used to see the intrinsic defect structure of materials. All other techniques like High Resolution Transmission Electron Microscopy (HR-TEM), Selected Area Diffraction (SAD) which reveals the atomic level image, interacts with the material and could induce defects in the structure.

Eventhough SnSe is extensively studied for thermoelectric behaviours, the surface properties of the materials are not explored much. STM studies on SnSe by Rhim and Kim reveal that both Sn and Se atoms arrange in a rectangular lattice with lattice parameters a=4.6Å and b=4.28 Å .Due to the puckered structure of SnSe, it is confirmed that the atoms observed on top are Tin. They reported a vacancy defect which is due to the missing of Sn atoms. [20]. Another paper which characterized Bismuth doped SnSe confirmed the rectangular lattice with Sn atoms on the top. Since Bi was substituted for Sn atoms, they could observe Bismuth with STM. This was further confirmed by DFT simulations [16].

SnSe doped with Pb atoms reveals one dimensional mid gap states at the odd number steps [21]. Pb-SnSe is reported to be a topological crystalline insulator [21]. Pristine SnSe is not a topological crystalline insulator due to its broken mirror symmetry in (110) direction. However epitaxial SnSe (111) films grown on top of $Bi_2Se_3$ are found to be a topological crystalline insulator. Here $Bi_2Se_3$ was deposited on $SrTiO_3$ by Molecular Beam Epitaxy technique (MBE). Then SnSe was synthesized on top of $Bi_2Se_3$ by M.B.E. STM was used to see how SnSe has grown on the substrate and to measure its layer thickness. Angle Resolved Photo Emission Spectroscopy (ARPES) data did confirm that SnSe has TCI behaviour when its thickness is 20nm or less .SnSe of thickness more than 20nm is observed to be in orthorhombic phase [22].

Even though the atomic structure of SnSe is investigated, the local electronic properties of the sample are not studied in detail. Defect investigation and Scanning Tunnelling Spectroscopy measurements have to be performed for a better understanding of the material.

In this present work, extensive exploration of local electronic properties of SnSe at the atomic scale is performed by STM at 77 K and at 300K. Large area scans were performed to understand the topographical features of SnSe single crystal at Pnma phase. Atomic resolution images have been taken to study the lattice arrangement and to determine the lattice parameters of the crystal. Detailed defects studies were performed to visualise various types of intrinsic defects in the crystal.

# CHAPTER II

# Methods

This section discusses the different experimental methods used at various stages of the project. Synthesis of SnSe and bismuth doped SnSe was done by Dr Luminita Harnagea

## 2.1 Synthesis

SnSe was synthesized using chemical vapour transport technique and bismuth doped SnSe was synthesized using Modified Bridgeman technique.

### 2.1.1 Chemical Vapour Transport

Chemical vapour transport is done in a furnace maintained with a temperature gradient. Reactants are taken in a quartz ampoule and kept in the hot side of the furnace (source). Temperature is maintained at 950ºC. Once they reach gaseous phase, they start circulating in the furnace. Crystallisation takes place in the cooler side of the furnace (sink) and it is maintained at 900ºC...

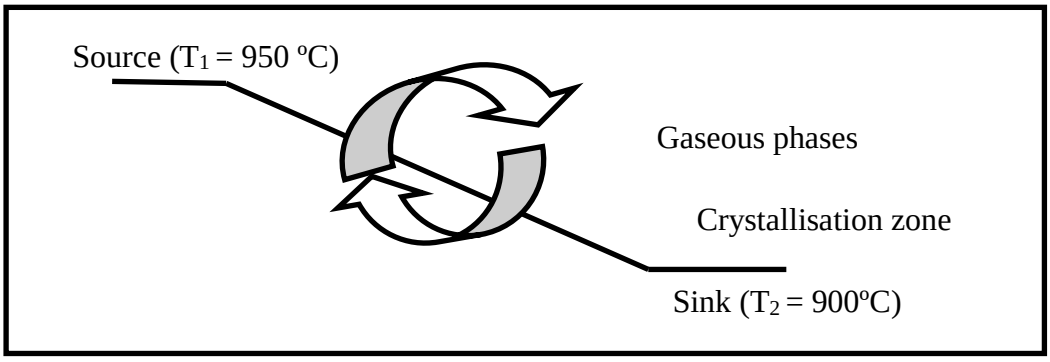


**Figure 2.1: Schematic diagram of Chemical Vapour Transport**

### 2.1.2 Modified Bridgeman technique

In this method, reactants in the crucible is melt completely in the hotter side of the furnace. Then melt is brought into contact with the seed present in the bottom of the crucilble. As the temperature in the bottom of the crucible goes below solidification temperature, crystallisation starts. Later, crucible is moved towards the cooler side and crystallisation gets completed there.

## 2.2 X-Ray Diffractometer (XRD)

XRD is used to identify the crystallinity and unit cell dimensions of a sample. In this technique, X rays are generated using a cathode ray tube upon applying high voltage of the order of kilo volts. The continuous electromagnetic radiation which is emitted by the cathode will go through a filter and becomes monochromatic X rays. These rays are further collimated and made to fall on the sample

Incoming X rays will interact with the sample and produces interference. Whenever interference becomes constructive, we get a peak in XRD corresponding to that. This is based on Bragg's law:

$$n\lambda = 2d \sin\theta$$

Where n is an integer, $\lambda$ is the wave length, d is the inter planar distance and $\theta$ is the angle of diffraction.

## 2.3 Field Emission Scanning Electron Microscope (FESEM)

FESEM is an imaging technique which uses electron beam as the source. Here electron beams are generated through Field Emission gun. Electron beams gets focussed and deflected by a set of electromagnetic lens and becomes narrow beam. These narrow beams will fall on the sample and ejects secondary electron from them. Secondary electrons ejected from the sample is collected and converted to a signal based on its velocity and angle. This signal is converted into the video and thus the images.

## 2.4 Scanning probe microscopy – AFM Atomic force Microscope (AFM)

AFM is used to visualise the topography of a sample. In this technique, a tip is attached to the cantilever which probe the sample surface. AFM Samples could be conducting or non conducting and measurement could be performed in air/liquid environment. AFM measures the force between tip and sample to create a topographic profile of the sample. Van der Waal's force dominates in this imaging as the tip sample separation is very less.

AFM could be operated in constant height mode or constant force mode. In constant height mode, we keep the distance between tip and sample constant and record the variations in force between tip and sample. Feedback loop is turned off in this mode. In constant force mode, force is kept constant and variations in height are acquired. This is done with the help of piezoelectric scanner which extends/contracts in Z direction to keep the force constant.

Three primary imaging modes of AFM are contact mode, non contact mode and intermittent/ dynamic mode. In contact mode, tip touches the sample surface and scans the area. It collects repulsive Van der Waal's force. This is advisable for liquid and soft samples only. In non contact mode, attractive force dominates. Since there is no physical contact with the sample, it does no harm to the tip/sample. However resolution is compromised in this mode. In dynamic mode/ intermittent mode cantilever does oscillate at a particular frequency and amplitude. At times, it taps the surface and goes back with variations in its amplitude and frequency. These variations are mapped and are used in creating the topography plot of the sample. Based on the force experienced between tip and the sample, there will be a deflection in the cantilever. This could be explained with the Hook's law, F= -kx where k is the spring constant and x is the deflection of the cantilever. Cantilevers of different spring constants are used for different modes. Laser detection is used to quantify the deflection of cantilever. Laser does fall on the back side of the cantilever and reflected light coming from the cantilever gets collected at the photo diode kept at the opposite side of the laser source.

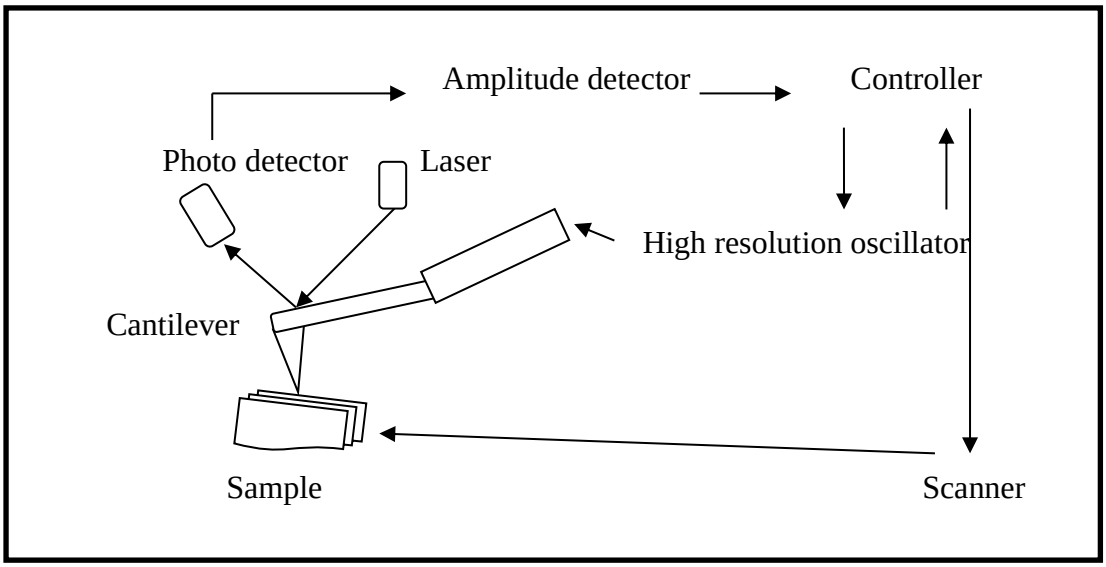


**Figure 2.2 Schematic diagram of AFM.[23]**

## 2.5 Theory of STM

### Concept of tunnelling [23]

Consider an electron wave with lesser energy than a barrier. Classically, it is impossible for the electron to penetrate into the barrier. But in quantum mechanics, there is a finite probability that electron can pass through. This phenomenon is called tunnelling.

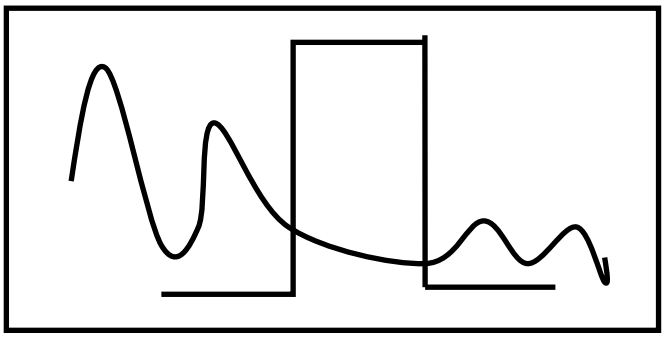

**Figure 2.3: Schematic diagram of one dimensional barrier [23].**

Solving the Schrodinger equation within the barrier gives the solution, $I \alpha e^{(-kx)}$ where $k = \frac{\sqrt{2m(E-V)}}{\hbar}$ and x is the distance between tip and sample.

E is the energy of electron wave and V is the barrier potential.

Consider the case of two electrodes: a tip and a sample. Bias applied between them causes a net tunnelling current to flow through them. Positive bias applied to the sample helps to probe the unoccupied states of the sample. Similarly, negative bias given to the sample probes its occupied states. One of the modifications of the tunnelling theory is given by Bardeen's approach.

### Bardeen's approach [23]

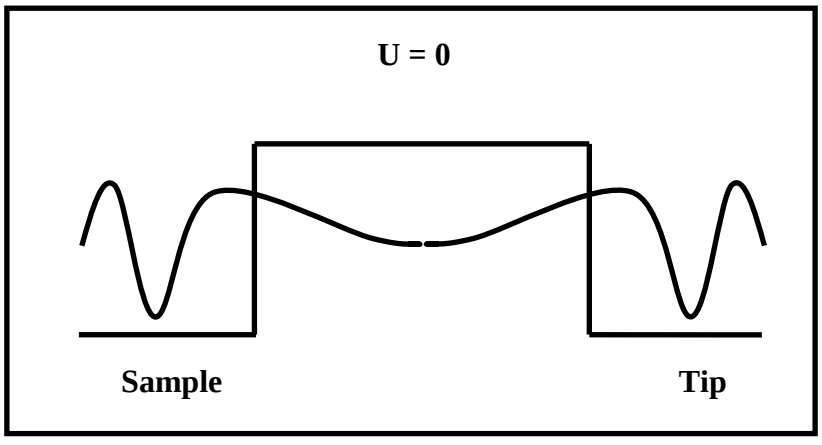


**Figure 2.4: Schematic diagram showing 2 electrodes kept apart [23]**

If the sample and tip are not close, there will not be any overlap of wavefunctions between them. Wavefunctions do decay into the vacuum in this case. For tunnelling, the separation between tip and sample has to be very small.

**Assumptions**

- Interactions between tunnelling electrons are not considered in low tunnelling regime
- Coupling between wavefunctions of tip and sample is neglected.

The wave function in the tunnelling regime is described using time dependent perturbation theory. When $t \Longrightarrow \infty$, wave function of the tip stays in stationary state. Potential of the tip is switched on adiabatically. The state in the tunnelling regime is described as the linear combination of wave functions of tip and the sample.

Expression of tunnelling current from Bardeen's approach is given by

$$I = \frac{4\pi e}{h} \int_0^{eV} \rho_s(Ef - eV + \varepsilon)\, \rho_t(Ef + \varepsilon)\, |M|^2 d\varepsilon$$

Where $\rho_s$ and $\rho_t$ are the density of states of sample and tip, $E_f$ is the fermi level, e is the charge of electron, V is the voltage, ħ is the Planck's constant and M is the tunnelling matrix

$$M_{\mu\nu} = \frac{\hbar^2}{2m} \int_{z=z_0} [\Psi_\mu \frac{\partial \chi_\nu^*}{\partial z} - \chi_\nu^* \frac{\partial \Psi_\mu}{\partial x}]\, dxdy$$

Ψ is the wave function of sample and χ is the wave function of tip

Expression for conductance could be approximated as

$$\left[\frac{dI}{dU}\right]_{U=V} \approx \rho_s(E_f + eV)\, \rho_t(E_f)$$

**Principle of STM**

**A** small bias is applied between a tip of known density of states and a conducting sample which is to be studied. STM helps to track the topography of the sample through the integrated density of states of the sample and tip. It helps to study the local electronic properties of the sample both above and below its Fermi level through I-V spectroscopy

STM imaging can be done in two modes: constant height mode and constant current mode.

**Constant Height Mode:** In this mode, separation between tip and sample is kept constant and the varying tunnelling current is measured. From the tunnelling currents mapped, we can trace back the topography of the sample whether it is a hill or a valley. This mode is not advised to use in an unknown sample as there is a possibility for tip crash.

**Constant Current Mode**: In this mode, tunnelling current between tip and sample is kept constant. Tip adjusts its height using a feedback loop, such that current is maintained throughout the scan.

**I-V spectroscopy**

This is a technique by which we can probe the local electronic properties of a material. In I-V spectroscopy, the separation between tip and sample is kept constant by setting at a particular current. Later voltage is varied and the corresponding tunnelling current is measured. Feedback loop is turned off during the entire process.

In our system, Scanning Tunnelling Spectroscopy (STS) measurement is done using Lock in amplifier. A frequency of 652 Hz and a modulation voltage of 20mV is set in the Lock in amplifier. A small AC component is added with the DC voltage that we apply. It is made sure that the frequency of the voltage is high so that feedback remains inactive. As we measure dI/dV from this, the effect of extra modulation gets vanished.

In order to eliminate the error coming from spectroscopy, more sets of data are taken and values are averaged out.

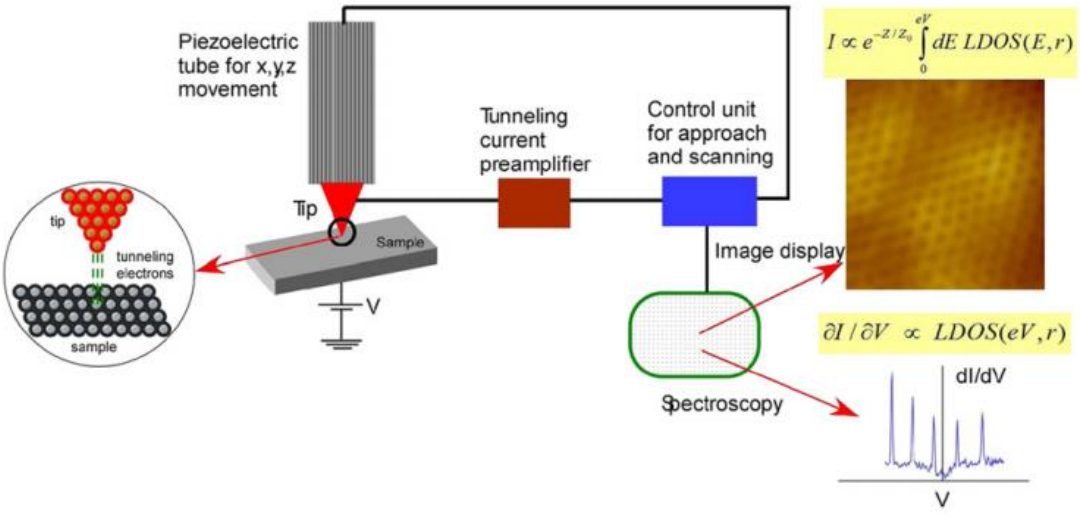


**Figure 2.5: Schematic diagram of STM electronics [24]**

Tunnelling current flowing between tip and sample is amplified in the pre amplifier as its magnitude is in the range of pico amperes. Later this goes into the control unit where it calculates the difference between set point current and the measured tunnelling current. Information will be passed to the piezo controller to adjust the height in Z direction such that constant current could be maintained ( in constant current mode). Similarly control unit applies voltage to piezo drive to do course movement and for scanning in x and y directions.

## 2.6 Ultra High Vacuum Low Temperature Scanning Tunnelling Microscope (UHV LT STM)

UHV LT STM comprises of Load Lock, Preparation Chamber and Low Temperature chamber. Conducting sample which is to be investigated is inserted through Fast Entry Lock/ Load Lock. Pressure of Load lock is in the range of $10^{(-6)} – 10^{(-7)}$ mbar and is measured using Pirani gauge. Preparation chamber has the provision for annealing, sputtering, crystal cleaving and depositing molecules. Since the sample preparation is done here, high vacuum is maintained in this part. Pressure is sensed using Ion gauge. Low Temperature (LT) chamber is where STM head is kept. Low temperature is maintained using liquid nitrogen.

### Ultra-High Vacuum (UHV)

Vacuum is defined as a region with gaseous pressure much lesser than the atmospheric pressure (1 atm). Vacuum could be classified into four types: Low vacuum (upto10 $^{(-3)}$ torr), Medium vacuum ($10^{(-3)} – 10^{(-6)}$ torr), High vacuum ($10^{(-6)}$ - $10^{(-8)}$ torr) and Ultra High vacuum (< $10^{(-9)}$ torr).

We use vacuum pumps like Rotary pump, Turbo molecular pump and Ion pump to achieve ultra-high vacuum. UHV condition helps to keep the sample away from contaminants and are suitable for samples which are air sensitive. Cleanliness of the sample is really important in STM studies as it is a surface sensitive technique. If there are adsorbents in the sample, this will affect the tip quality which affects both imaging and spectroscopy.

The number of particles in Ultra high vacuum environment can be estimated using Ideal gas law, PV= NRT where P is the Pressure, V is the Volume, N is the number of moles, R is the universal gas constant and T is the temperature.

N/V * Avogadro number (Na) = P/RT = $10^{(-7)}$ Pa/ (8.24 × 300K) = 2.5 × $10^{(13)}$

The number of particles in ambient conditions is $2.5 \times 10^{(25)}$.

This huge difference in the number of particles explains how much UHV environment helps to keep the sample contaminant free

**Rotary vane pump**

Vacuum of $10^{(-2)}$ to $10^{(-3)}$ mbar can be achieved using a Rotary vane pump. In this pump, there is a stator, a rotor and a vane(blade) connected to springs. Residual gas will enter through the inlet of the pump. The vanes which are connected to the rotor does rotate, transport and compress the gas and release it outside in atmospheric pressure through the outlet. Since the pressure difference between inlet and outlet is quite high, distance between rotor and stator are kept small like 0.025mm.

Oil is used in sealing the inlet and outlet of the pump. If the oil is contaminated, it will affect the performance of the pump and reduce its lifetime.

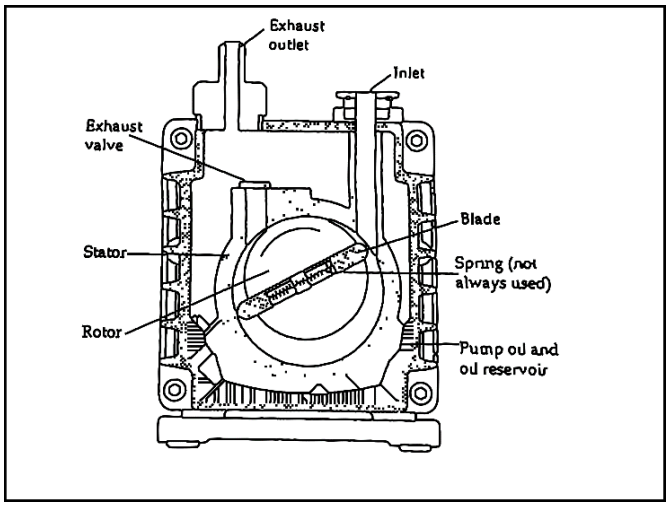


**Figure 2.6: Schematic diagram of Rotary vane pump [25]**

**Turbo molecular pump**

In this pump, we have rotors and stators arranged closely. When gas molecules collide with the rotor, which rotates at very high velocity, it acquires extra momentum. Later these molecules will be pushed to the stator and further to the exhaust. If the gas molecules lose energy from the collision, it won't be able to reach stators. In this case, removing the residual gas becomes tricky. Hence using turbo molecular pump is not advisable below 10 torr. So we use a backup pump, which is a rotary vane pump for operating turbo molecular pump. Rotary pump will start running initially and creates rough vacuum before turbo molecular starts to run. Rotor and

stator must be very close as it has to overcome the mean free path of the molecules. Pressure of around $10^{(-9)}$ mbar could be made using this pump.

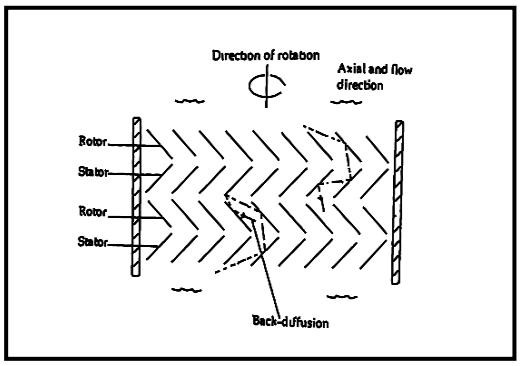


**Figure 2.7: Schematic diagram of Turbo molecular pump [25].**

**Ion pump**

Electrons are produced through electric discharge between two electrodes. High magnetic field coming from the permanent magnet will cause these electrons to revolve in circular motion. These electrons will be pulled towards the anode. On the way to Anode, electrons do collide with the residual gases/molecules, and ionise them. Thus residues become positive in charge and will be attracted towards the cathode. These molecules could be embedded in the cathode or it will cause the ejection of an electron from cathode. If the residue ejects an electron from cathode, it becomes negative in charge and move towards anode assembly. Current flowing between these electrodes is an indirect way of determining the number of molecules present in the system. Ion pump is used to improve the pressure in Preparation chamber and Low Temperature chamber of UHV LT STM.

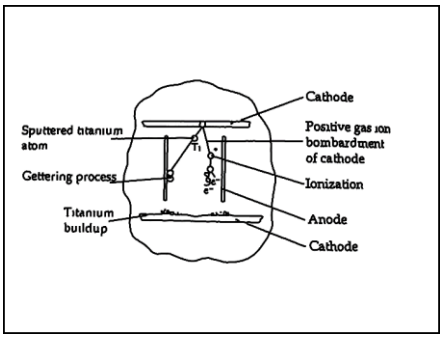


**Figure 2.8: Schematic diagram of Ion pump [25].**

**Titanium Sublimation pump (TSP)**

High current is passed through the filament which causes Titanium to sublime. Titanium will form a thin layer on the walls of the chamber. Since fresh Titanium is reactive, it will react with the residues. Later this will be taken out using Turbo molecular pump or Ion pump. Once Titanium is not clean, it will not be as reactive as before. So we need to fire TSP at regular intervals of time. TSP is used in preparation chamber and in LT chamber to improve the pressure.

**Gauges for measuring Pressure**

There are two types of gauges used in measuring Pressure in our system: Pirani Gauge and Ion gauge

**Pirani gauge**: This is a type of thermal conductivity gauge. In this gauge, Platinum will be heated initially by passing current through it. The molecules present in the system will go collide with the filament and reduces the heat of the filament. If there are fewer molecules present, heat of the filament will fall down slowly. By measuring the heat loss of the filament, we are in a way calculating the number of particles in the system.

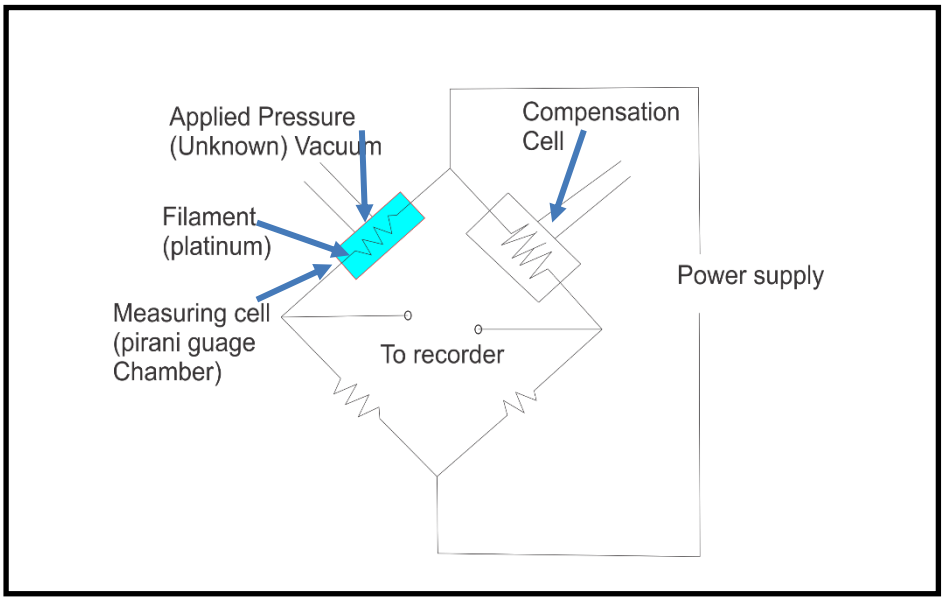


**Figure 2.9: Schematic diagram of Pirani gauge**

**Ion gauge**: In this method, electrons are emitted from the filament which acts as the cathode and get attracted towards the Grid. These electrons collide with the residual gases/molecules making them lose their valence electron. Positive ions formed like this are collected at the positive grid/ Anode. Current detected in this way is a measure of number of particles in the system and hence a measure of the vacuum.

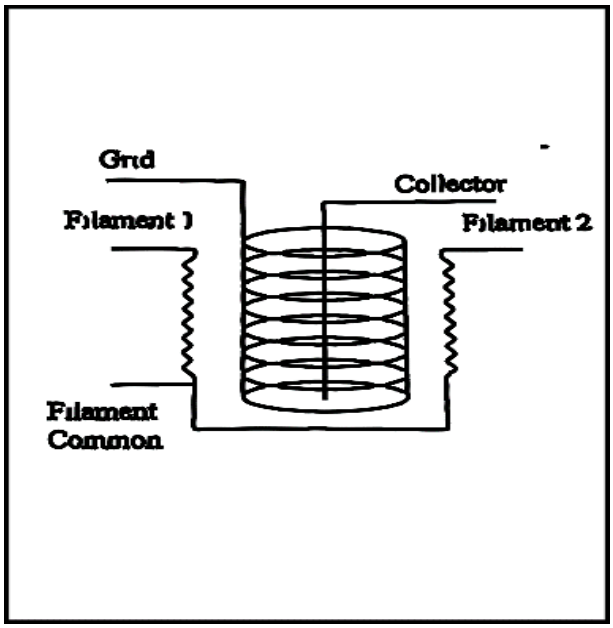


**Figure 2.10: Schematic diagram of Ion gauge [25].**

**Low Temperature (LT) Chamber**

**LT** chamber is comprised of two cryostats, Scanning Tunnelling Microscope and carousel where samples rest. Inner and outer cryostats present in the chamber are filled with liquid Nitrogen/ liquid Helium based on our need of temperature. Outer cryostat works as a thermal shield for the inner one and STM is kept inside a copper cup attached to the inner cylinder. Thus lower temperature could be maintained throughout the experiments. Similarly eddy current damping assembly is also attached to the inner cryostat.

**Locking mechanism**

There are three locking mechanism for our system which can be controlled using a lever attached to the topmost part of LT chamber.

**Cool down position**: In this position, STM is in touch with the cryostats and thus achieve low temperature faster. This is used whenever we insert/remove sample or tip.

**Bake out position**: This position is used when LT is getting baked. Here SPM is fixed firmly, and springs are completely supported.

**Tunnelling position**: This position is used for measurement. Here STM is hanged freely using springs.

**Preparation chamber**

In this part, we have provision for annealing the sample, sputtering it, cleaving the crystal and depositing molecule. Ultra High Vacuum is maintained so that sample surface is kept clean. Annealing could be done in two different ways: Direct Heating and Indirect heating. In direct heating technique, current is passed through the sample and it heats the sample according to Joule's law. In indirect heating method, current is passed through a tungsten filament which in turn heats up the sample via resistive heating.

Crystals could be cleaved in situ in ultra-high vacuum conditions in this chamber. Crystal cleaver consists of a stamp, onto which we press our crystal. Crystal leaves its topmost layer on the stamp, exposing a fresh surface for studies.

Gas chambers are connected to the preparation chamber, where we could use argon for sputtering and oxygen for deposition. Valves of these gas chambers are connected directly to the turbo molecular pump. So if there is an excessive flow of gases, it could be removed by turbo molecular pump.

Molecular evaporators are connected to this chamber. Molecules are filled inside crucibles which are heated to evaporate the sample and get deposited in the surface of interest. Thermocouple is connected to the crucible which gives an estimate of the temperature during deposition. If the temperature is more than 300°C, it could be estimated using a Pyrometer.

**Load Lock**

This is the part which has direct communication to outside.

For inserting a sample/tip: Vent the load lock using Nitrogen gas. Insert the sample/tip. Tighten the screws properly and switch on turbo molecular pump. Once it achieves a pressure of $10^{(-7)}$ mbar, sample/tip could be transferred to the preparation chamber.

Pressure in load lock is measured using Pirani gauge.

**Magnetic probes (Magprobes)**

Magprobes are manipulators which help us to transfer sample inside the system. There is a magprobe which connects Load lock and Preparation chamber. Whenever the pressure variation is comparable, valve between these two could be opened and transfer can be done. Magprobe which connects between preparation chamber and LT chamber has two rods. These rods need a support, and it can open its jaw only if the support is proper. It will make sure that the transfer is made without any issues like losing the sample.

**Vibration Isolation**

Vibration isolation in STM experiments is crucial as we are dealing with variation of hundreds of picometer in Z direction. If an external vibration affects the system, STM head will oscillate due to that frequency. This might lead to the crashing of tip and thus losing a very sharp edge. Crashing a good tip affects image quality and thus our time.

**Provisions in our system**

- Spring suspension: LT STM stage is suspended using three soft springs. Resonance frequency of the spring comes around 2Hz. Eddy current damping mechanism is achieved using a ring of metal damping U profiles which cover around STM stage. This is used to obstruct the vibrations in this suspension system.
- External vibration isolation using sand.

**Tip preparation**

A sharp tip is mandatory to give an atomic level image from. Usually people use Platinum Iridum (Pt-Ir) and Tungsten for making STM tip. Tip from Pt-Ir is made by a mechanical cut and Tungsten tip is made from chemical itching. NaoH solution of 3.5 M is used for the chemical etching process. A voltage range between 4-5V works

**Set up for chemical itching**

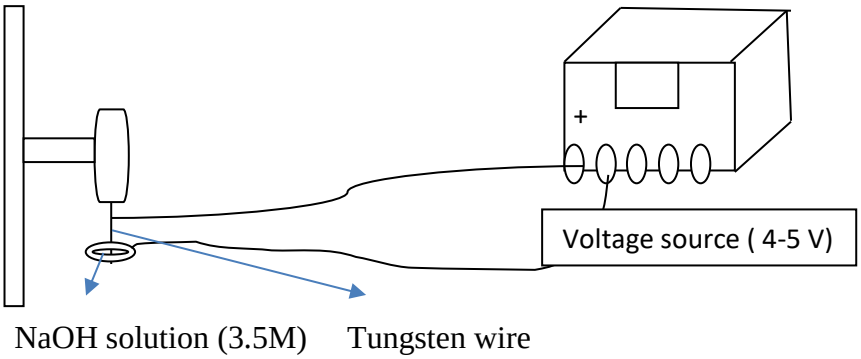


**Figure 2.11: Schematic diagram for tip preparation.**

## 2.7 Methods for exfoliation

**Mechanical exfoliation:** A scotch tape of high adhesiveness is pressed on top of a layered material of interest. A thicker flake of the crystal will be transferred to the tape, as its adhesion with the sample is strong enough to overcome the Van der Waal's interaction. The obtained flake is pressed many times on the tape to make it thin. Once it becomes really thin, it is transferred to the substrates like silicon, silicon dioxide, gold coated mica for further studies. Flakes of different sizes could be obtained if adhesiveness, speed of transfer, substrate are varied.

In order to reduce the number of thicker flakes from getting transferred to the substrate and to reduce the remnants coming from the scotch tape we could use Poly Dimethyl Siloxane stamp in the final transfer step. Once the layers are made thin in the tape, it is transferred to the stamp directly rather than the substrate. Later, transfer is done between PDMS stamp and the substrate of interest.

Exfoliation technique is used to expose a fresh surface for layered materials (crystals)

**Heating**: If we heat the crystal, layers could be separated easily. So this step could be incorporated prior to the usual Scotch tape technique

**Ultra-sonication**: In this method, layered material of interest is added to a solvent of comparable surface energy and ultra-sonicated. The heat energy coming from the process is

adequate enough to overcome the weak Van der Waal's interaction between layers and hence layers get separated

**Mechanical exfoliation to produce few layers of SnSe**

Mechanical exfoliation technique was used to produce few layers of Tin Selenide. Substrate used were gold coated mica and $SiO_2$ coated Si wafer. After the whole procedure of exfoliation, flakes were observed under Optical Microscope. Since flakes of various thickness would produce different contrasts based on Fresnel's law on $SiO_2$ wafer, we will be able to observe whether few layers are present or not. Later, flakes of interest will be traced in Atomic Force Microscope (AFM) for investigating its height from the substrate.

## 2.8 Optical Microscope

Optical Microscope uses visible light and a set of magnifying lens to visualise our sample of interest. A camera is attached to the microscope, which enable us to observe things directly on the computer screen without using an eye piece. Magnification range of the used objective of the microscope- Zeiss varies from 5 X- 50 X. However samples below few hundreds of nanometre could not be observed in Optical Microscope-Resolution of a microscope is defined using its wavelength and Numerical aperture (N A) of its lens. It is given by $\lambda/2 \times (N.A)$

## 2.9 Photolithography

Flakes that we obtain from exfoliation come in few microns length. Even though it is easy to visualise these flakes in Optical Microscope, tracing these in AFM is tricky. One way to work around this hurdle is to pattern the substrate/design markers for the substrate. Photolithography is a technique by which we can make pattern on the substrate using light. I prepared Gold grids with labels, so that we can note this marking in Optical Microscope and trace the same region in AFM.

**Steps for Photolithography**

- Wafer cleaning: wafer has to be cleaned well using soap solution followed by ultrasonication with isopropanol, acetone and distilled water. Before starting the patterning, wafer has to be dried properly.
- Photoresist is coated using spin coating method. A speed of 3000-6000 rpm is used for a time duration of 10s
- Wafer is baked for a minute.

- A suitable lens is chosen based on the size of pattern we need. Wafer is kept under the lens and pattern is transferred to it.
- Once the patterning is done, Sputtering/ Physical Vapour Deposition is used to coat Gold on the patterned wafer.
- To remove the photoresist, a developer is used
- To remove the extra gold, wafer is washed using acetone.
- After this, we will be able to see the pattern covered in gold. Wash the wafer with distilled water in the final step, so that there won't be any film of acetone left.

## 2.10 Sputtering

In this method, energetic particles are made to fall on gold substrate. Kinetic energy of incoming ions should be large enough to eject the Gold atoms from its surface. Since this is performed in vacuum, kicked out atoms will be directed to the substrate of interest ($SiO_2$) through ballistic transport. By controlling the pressure and time of deposition we can tune the uniformity of the thin film of Gold on $SiO_2$ wafer

## 2.11 Physical Vapour Deposition

Gold is heated such that it will vaporise and gets deposited on $SiO_2$. Thermal Vapour Deposition is done at vacuum condition. Quartz is kept to monitor the extent of deposition in the system. By tuning the pressure, temperature and time we can optimise the uniformity of the Gold film on the substrate.

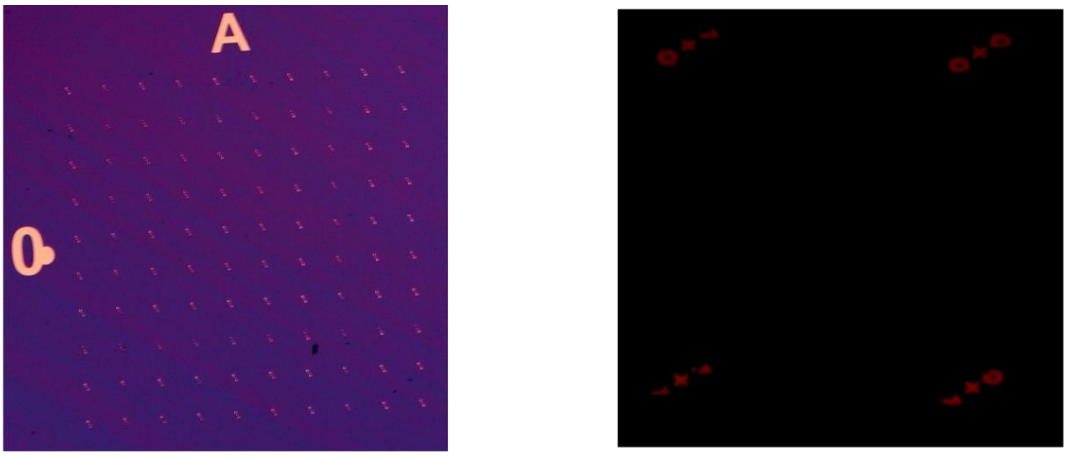

Lower Magnification Optical Image– 10X  High Magnification Optical image- 50X

**Figure 2.12 Optical image of photolithographic grids**

# CHAPTER III

# RESULTS AND DISCUSSION

This chapter deals with the results and discussions of the data taken. Characterisation techniques involved are X ray diffraction, Optical Microscope, Atomic Force Microscope and Scanning Tunnelling Microscopy. STM studies of pristine SnSe were performed at 77K and at 300K. Two different pieces of the SnSe crystal was used respectively for the STM studies in room temperature system and in the UHV-LT system. XRD & SEM characterization are done by Luminita Harnagea. These are added here with her permission.

### 3.1 X ray diffraction pattern of SnSe

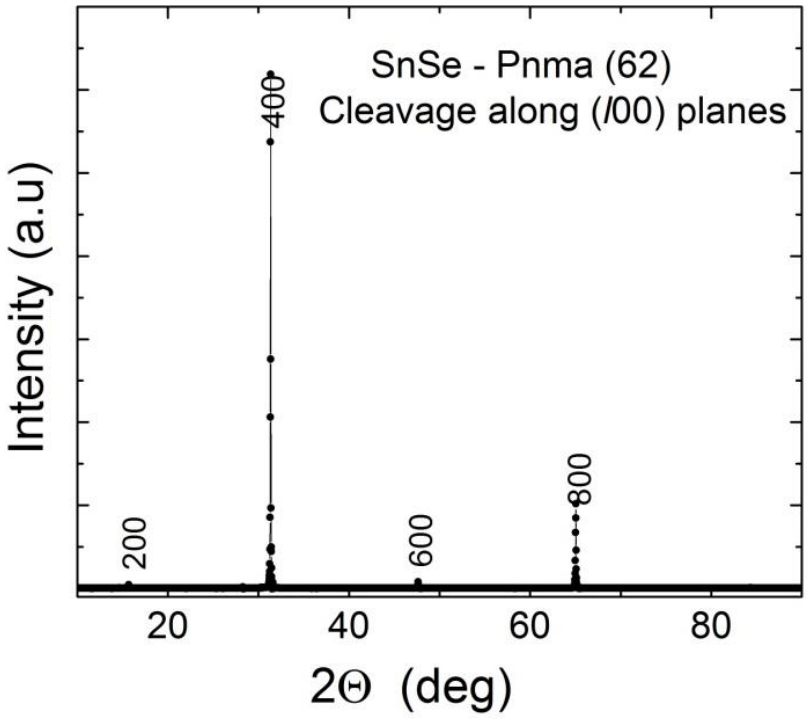


**Figure 3.1 : Powder X ray Diffraction pattern of pristine SnSe**

The peak at (400) is of highest intensity and it confirms that the crystal grows in (100) plane [20 ].

XRD pattern matches with the Pnma phase of SnSe with lattice parameters a= 1.145 nm b= 0.4145 nm and c = 0.441 nm. SnSe is synthesized at a temperature of 950ºC and thus it forms in the more symmetric Cmcm phase. But since Cmcm to Pnma phase transition is reversible, SnSe stays in orthorhombic Pnma phase at ambient conditions. If high temperature XRD could be taken, Cmcm phase could be observed.

### 3.2 Scanning Electron Microscope and Atomic Force Microscope image of pristine SnSe

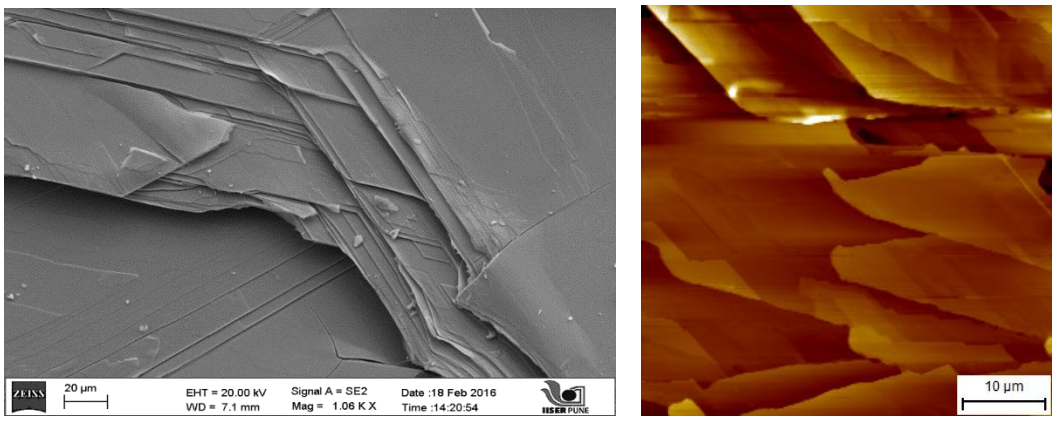


**Figure 3.2 (a) shows the SEM image of SnSe (b) shows the AFM image of SnSe.**

Figure above shows the topography of SnSe single crystal using Scanning Electron Microscope and Atomic Force Microscope. It is observed that there are lots of layers present in the material. SEM and AFM image shows the same features in the material. This helps to confirm that the growth of this layered crystal is layer by layer

### 3.3 STM image of pristine SnSe at room temperature

SnSe single crystal was exfoliated using Polydimethylsiloxane (PDMS) stamp. PDMS is a viscoelastic stamp which has lesser adhesiveness compared to usual adhesive tape (Scotch tape). The freshly exposed surface of SnSe was probed using mechanically cut Platinum Iridium wire.

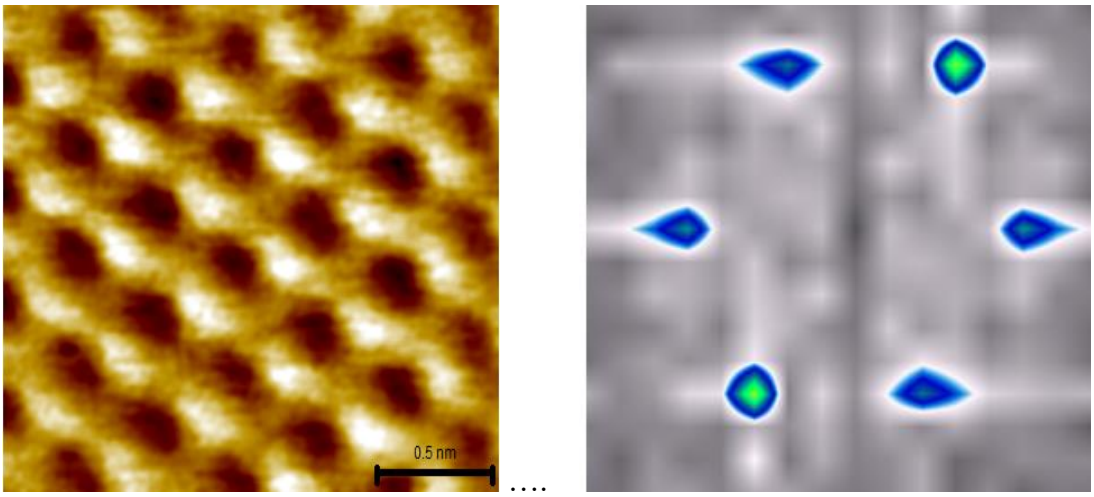


**Figure 3.3: (a) STM image of SnSe at room temperature with V = 0.5 V and I = 500pA**

**(b) Fast Fourier Image of STM image given at (a)**

Figure above shows the atomic arrangement of SnSe in real space and in fourier space. This is clearly a hexagonal lattice in (111) plane.The lattice parameters calculated from the STM image gives b= 3.98 ± 0.02 Å and c= 3.7 ± 0.01 Å .Fourier analysis gives the values b and c as 3.92 ± 0.09 Å and 3.88 ± 0.07 Å respectively.

### 3.4 I-V Spectroscopy at Room Temperature

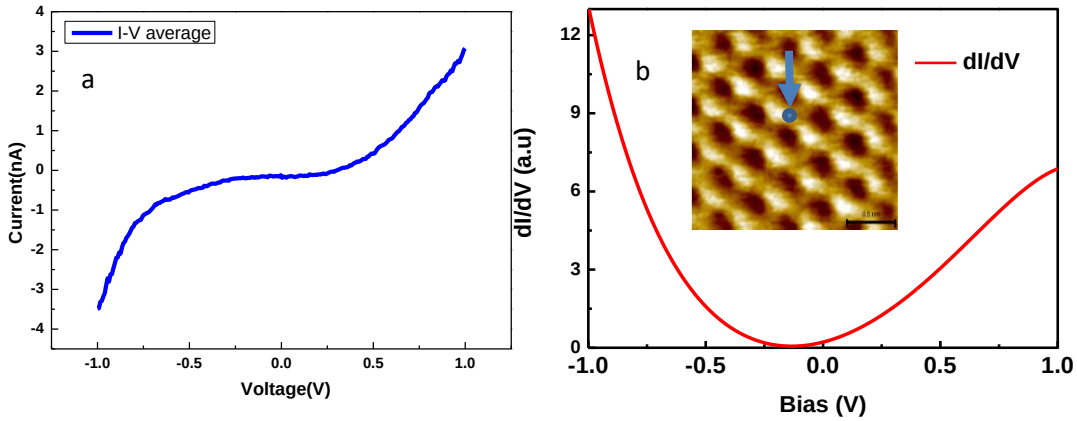


**Figure 3.4: (a) I V spectroscopy at room temperature. (b) dI/dV vs Voltage at room temperature**

I V spectroscopy of atoms from -1V to 1V voltage is given in the plot. This is an averaged plot of STS spectroscopy performed over various atomic sites. Tunnelling current obtained for various voltages seems to be in the same trend for different atomic sites. Figure 3.4 (b) shows the dI/dV curve, numerically differentiated from I V curve in the voltage range from -1V to 1V. This shows a band gap of around 0.25 eV

### 3.5 STM image at 77K

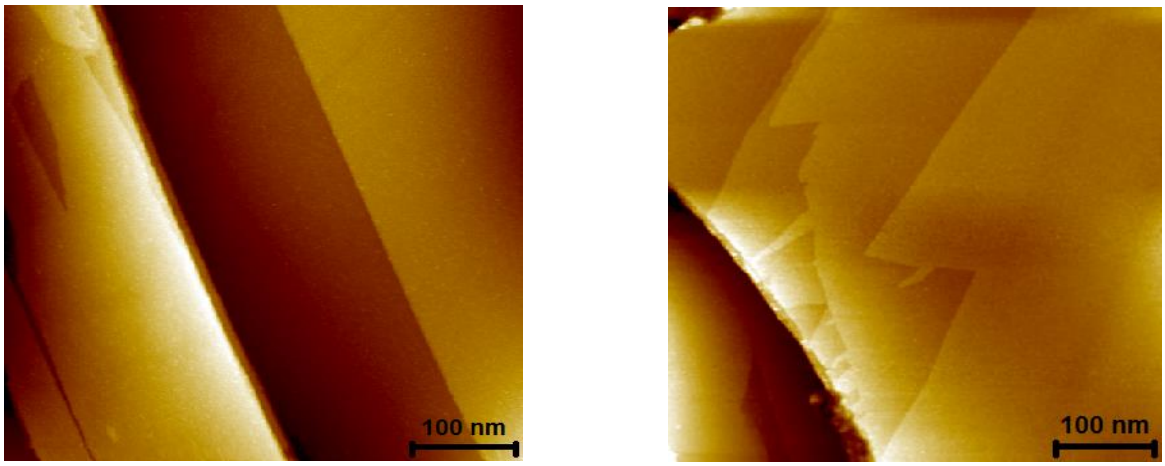


**V = 3.5 V I = 30 pA** **V = 2 V I = 80 pA**

Figure 3.5: Large area STM images of SnSe showing atomic steps.(a) V = 3.5V, I = 30pA and (b) V = 2V, I = 80 pA .

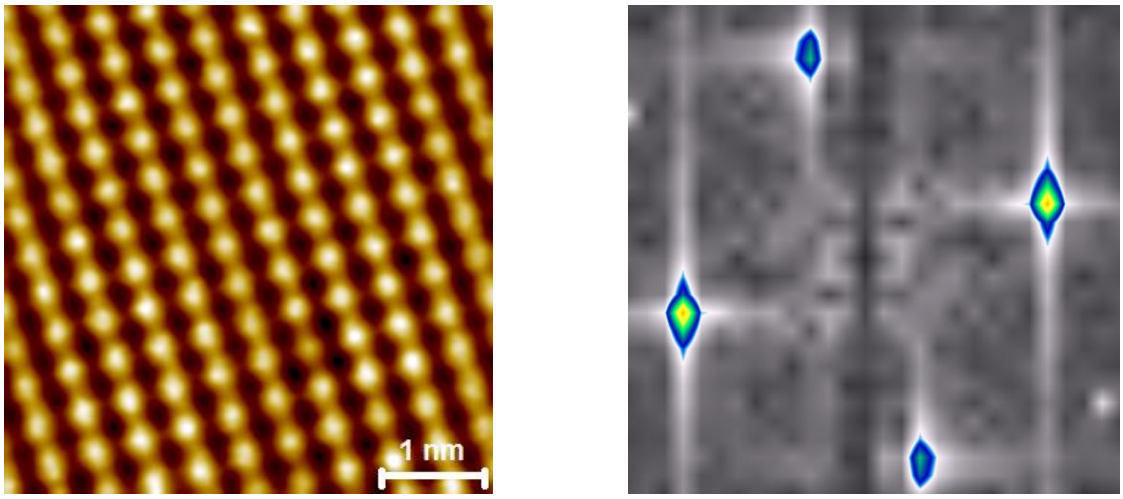


**Figure 3.6: (a) STM image showing atomic arrangement with V = -3.5V and I = 80 pA. (b) Fast Fourier Transform image of the STM image given at (a)**

Figure above shows the atomic resolution image in (100) plane with V = -3.5 V and I = 80 pA. Sn atoms which is slightly protruded above Se atoms are observed as the bright spots in this image. Similarly, Se atoms also forms a rectangular lattice which are the dark spots observed. Figure 6 (b) shows the fast fourier transform image of the atomic resolution image given at (a).

Here we can see the four dominant points which confirms the rectangular lattice of SnSe single crystal.

The lattice parameters found from the STM image is b= 4.15 ± 0.03 Å and c = 4.47 ± 0.03 Å. Lattice parameters found from the fast fourier transform image gives b = 4.02 ± 0.07 Å and c = 4.46 ± 0.06 Å

### 3.6 Scanning Tunnelling Spectroscopy at 77K in (100) plane

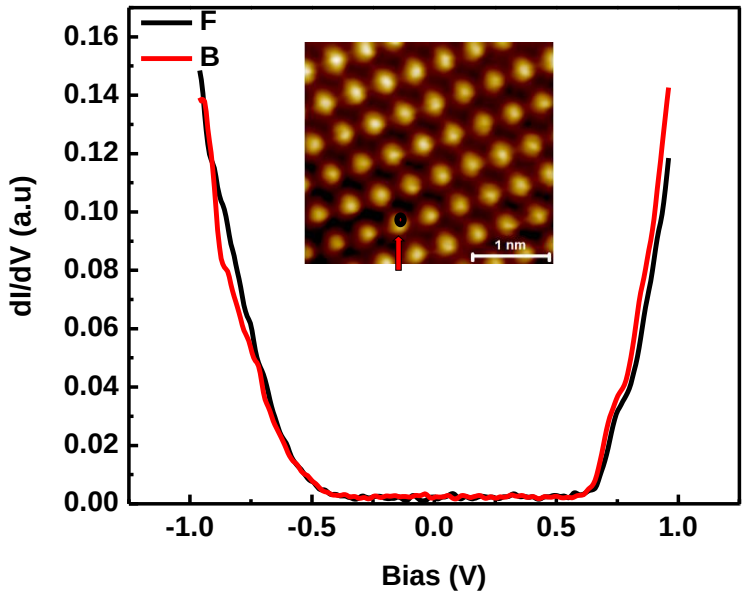


**Figure 3.7: dI/dV curve of Sn atoms in (100) plane from -1V to 1V. B corresponds to backward scan and F corresponds to forward scan**

The plot of conductance with the voltage range from -1V to 1V is shown above. We can observe a flat region in the curve which corresponds to the band gap of SnSe. It comes around 1eV for the single crystal SnSe in Pnma phase. [26] This is comparable with the reported band gap value of 0.85eV measured in a powdered SnSe sample [14].

## 3.7 Defects in SnSe

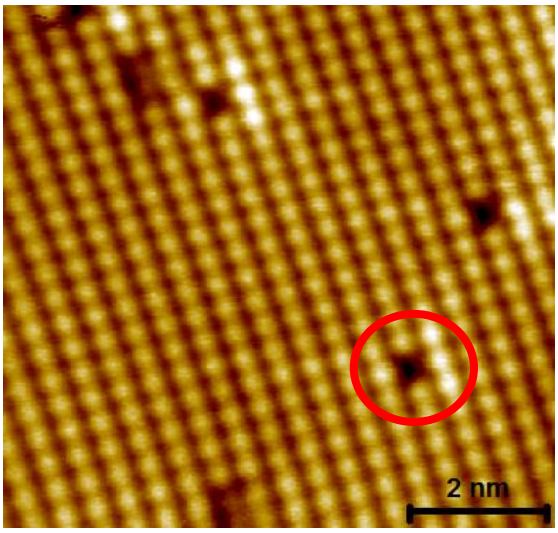


**V = -3.5, I = 80pA**

**Figure 3.8: atomic resolution image with parameters V = -3.5 V and I = 80pA.**

Figure 3.8 shows few black coloured points where the integrated electron density is less. These are vacancy defects coming due to the missing of Sn atoms. It can be clearly observed that there is a particular pattern formed by these defects.

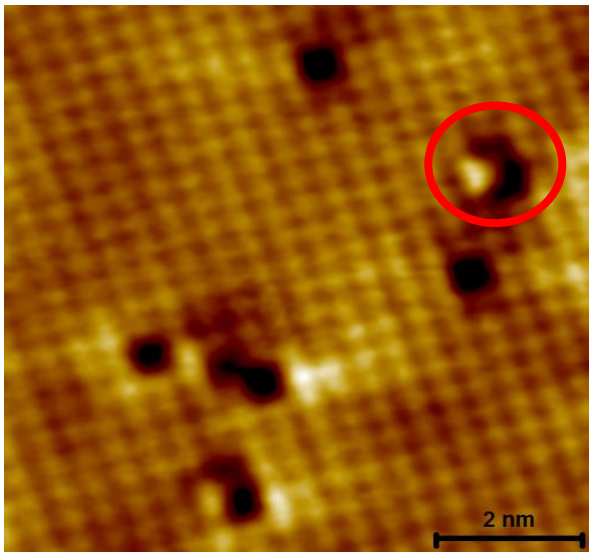


**Figure 3.9 : STM image showing atomic arrangement with V = -2V and I = 100 pA**

Figure 3.9 shows the atom level arrangement of Sn atoms with V = -2 V and I = 100 pA. We can observe two C shaped defects in this area along with the missing Sn atoms. C shaped defect covers the place of roughly three Sn atomic sites.

**Lattice mismatch**

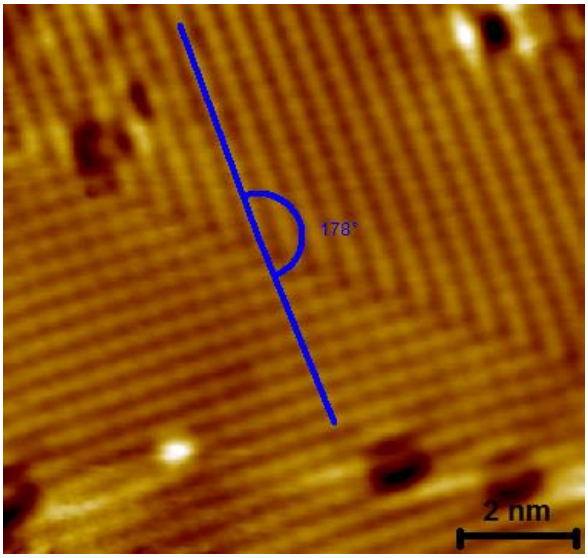


**Figure 3.10 (a): STM image shows atom level arrangement of Sn atoms with V = -1.8V and I=60pA.**

The lattice mismatch that we observe here could be due to the twin boundary of single crystal. Twin boundaries can occur, when two SnSe crystal grows into each other. The atoms in the boundary are shared by both of the lattices. Most of the times, these defects are reversible. These boundaries could be eliminated if we apply pressure along a direction in the crystal.

The angle deviation between the upper half and the lower half of the boundary is 2º. It is clearly observed that boundary acts as a mirror of symmetry.

### 3.8 Height variations in defects

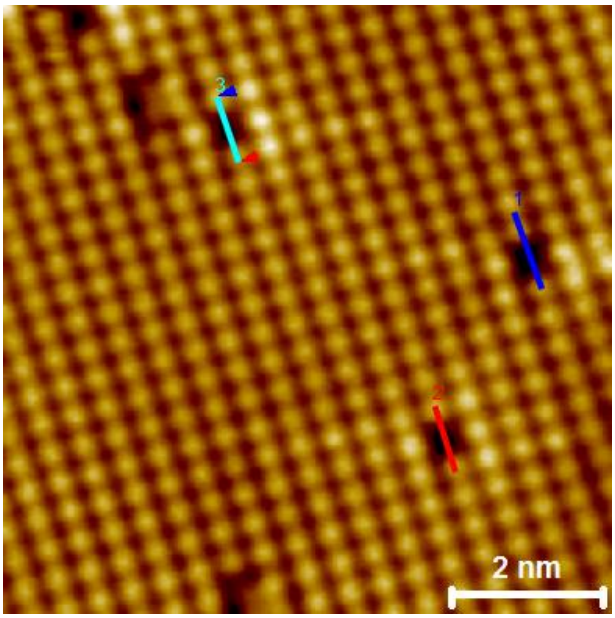


**Figure 3.11 (a)- STM image showing vacancy defects due to missing of Sn atoms. (b)-(d) Height profile of the vacancies observed**

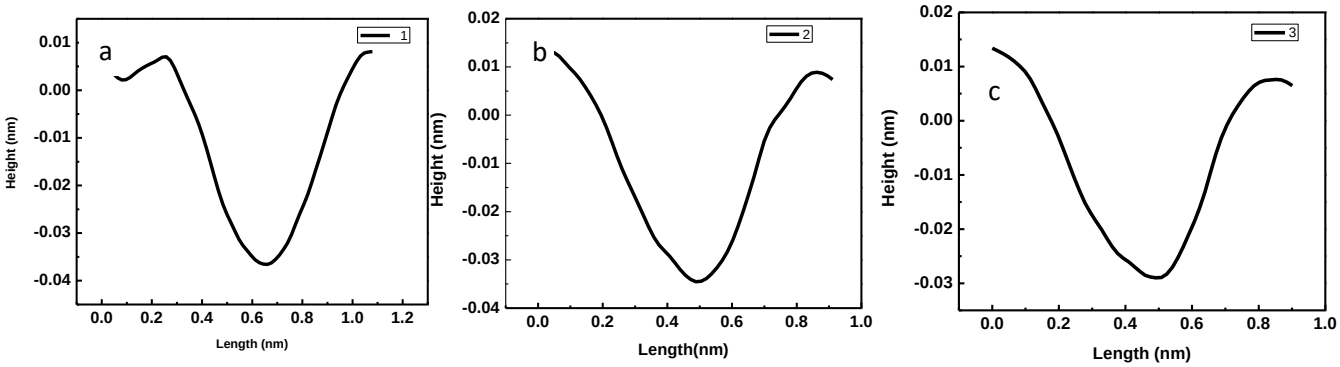


**Figure 3.12 (a)-(c) shows the height variation of the defects. A depth of 0.03 nm is observed.**

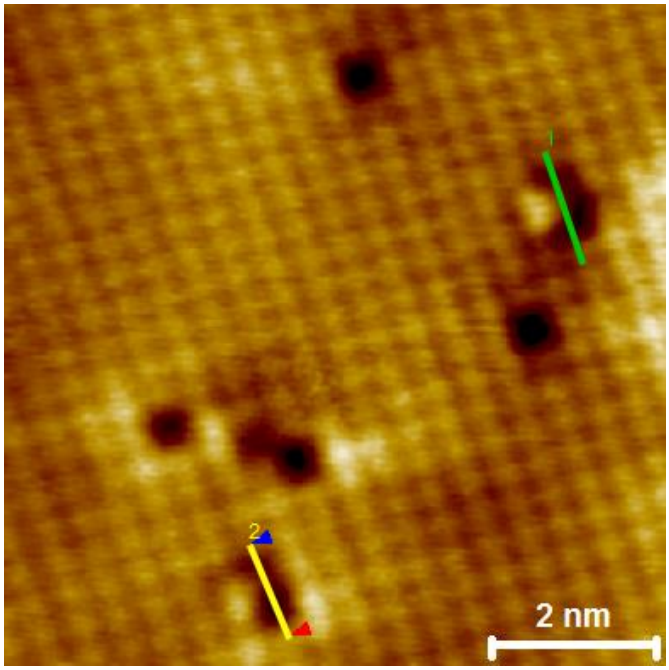


**Figure 3.13 (a) STM image showing a defect**

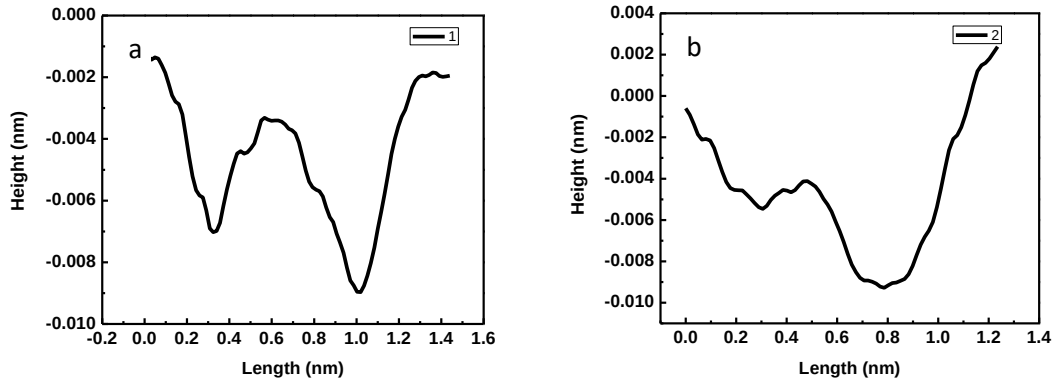


**Figure 3.14 (a)- (b) shows the height variation of these defects.**

Two dips are observed in these kind of defects unlike from the Sn vacancy defect observed before. The depth of the first dip is around 0.006 nm and the height variation of the second dip is around 0.008nm.

### 3.9 Spectroscopy performed on Sn vacancy in (100) plane

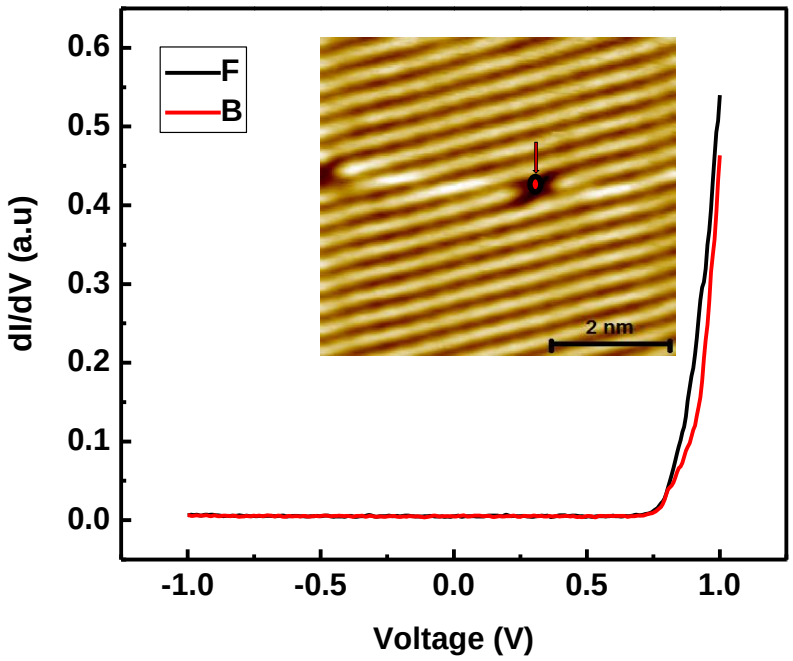


**Figure 3.15: dI/dV curve taken on a Sn vacancy**

Figure 3.15 shows a STS spectroscopy data performed on top of a Sn vacancy. Trend of this curve seems to be different from the other spectroscopy datas. There is a rise in the number of states available for tunnelling after 0.75 V.

It is expected to have a different local electronic behaviour at defects from that of atomic sites. This set of data was performed on three different sites and the curve is not varying with respect to the positions.

This is a primary result . More spectroscopic measurements will be performed in this direction.

Similarly, it is expected that the dI/dV curves would behave differently at the C shaped defect.

### 3.10 AFM image of Bismuth doped SnSe

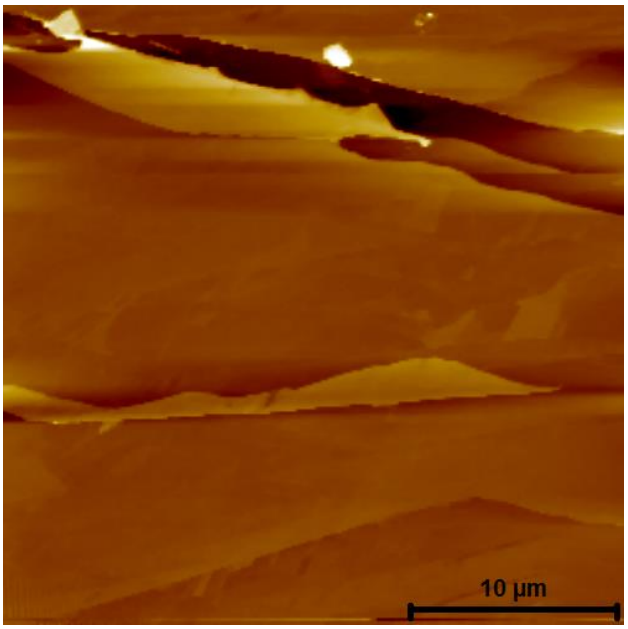


**Figure 3.16: AFM image of doped SnSe**

Figure 3.16 shows the AFM image of bismuth doped SnSe. The topography seems to be similar to that of pristine SnSe. Layers can be observed from this image, which confirms the layer by layer growth of the crystal.

### 3.11 STM image of Bismuth doped SnSe at 300K

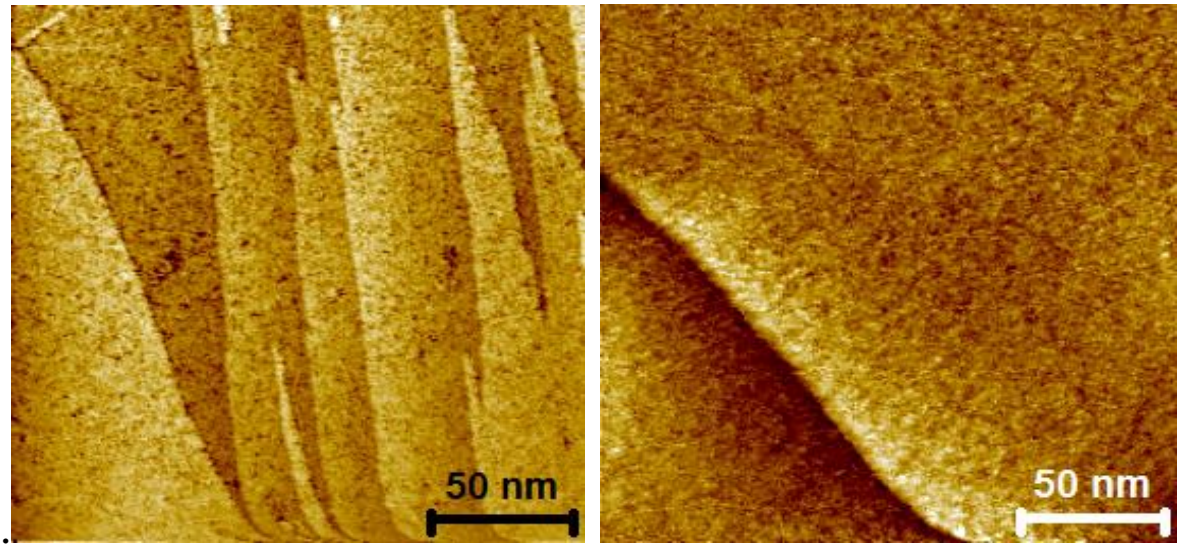


**(a) V = 2 V I = 1 nA** **(b) V = 2V I = 0.9 nA**

**Figure 3.17 (a)-(b) STM image showing the large area scan.**

It could be observed that the surface of bismuth doped SnSe is not very smooth. Efforts were made to improve the flatness of the surface using micro mechanical cleavage technique. But not much difference could be obtained by this method. An atomic resolution image obtained from the above area is shown below:

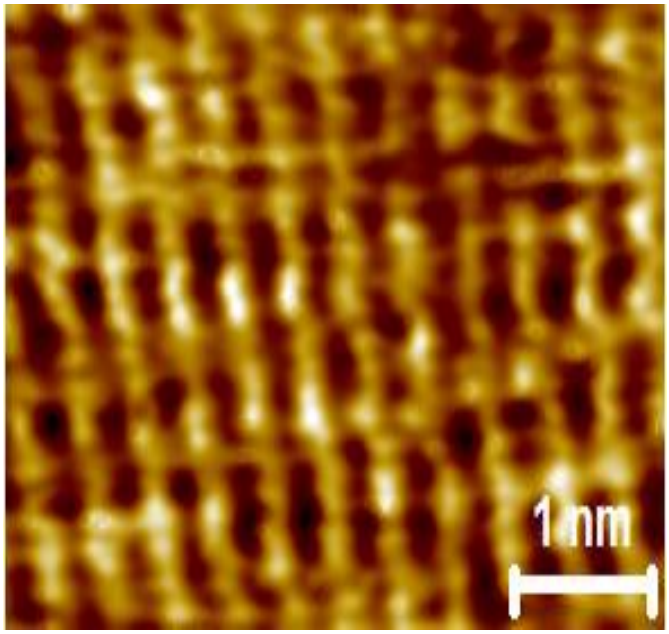


**Figure 3.18: (a) atomic resolution of bismuth doped SnSe**

Bismuth atoms has a different electron density compared to that of Sn atoms. Since, atoms could not be resolved well, signature of bismuth atoms are not found in this image. The sample has to be cleaned using annealing and sputtering to improve the flatness of the sample.

### 3.12 I-V spectroscopy of bi doped SnSe

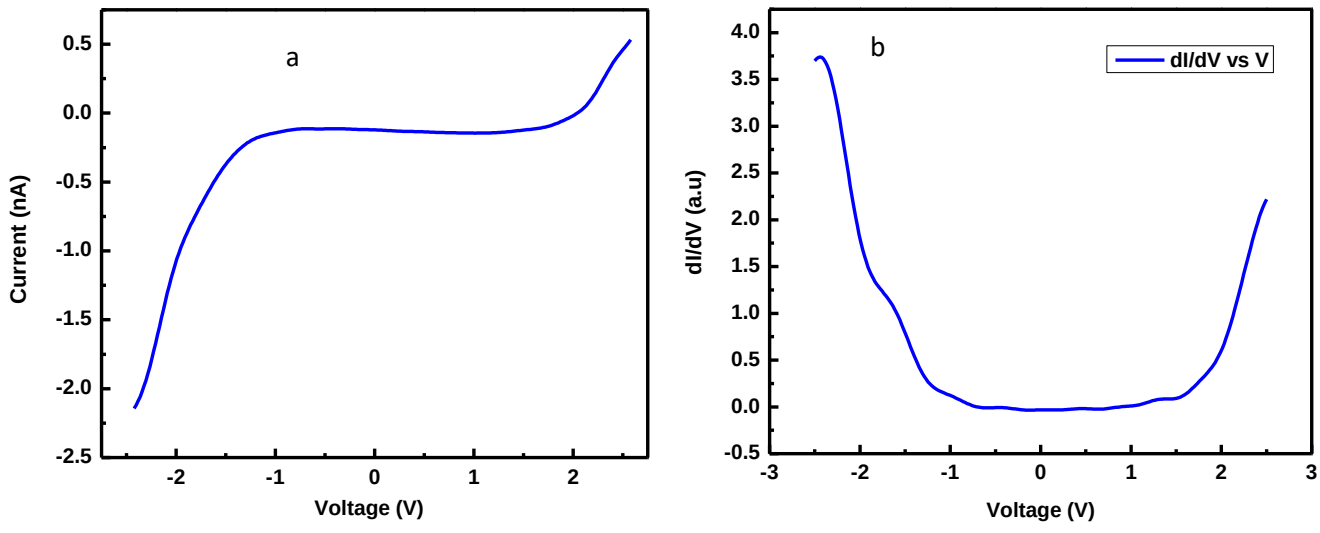

Figure 3.19 (a) shows the I-V characteristics of bismuth doped SnSe performed from -2.5 V to 2.5 V at room temperature. It is observed that the area is quite flat between -1V and 1.5V. Figure 3.19 (b) shows the dI/dV curve of bi doped SnSe performed between -2.5 V to 2.5 V. It can be observed that the bandgap of doped SnSe is different from that of pristine SnSe. Here a gap of around 1.5 eV is observed. This increase in bandgap could be due to the Burstein - Moss effect. When SnSe is doped with bismuth (Bi) atoms, extra electrons coming from Bi occupy the conduction band of SnSe. Since the crystal is heavily doped with 10% of bismuth atoms, it will lift the fermi level inside the conduction band. So for the excitations of electrons from valence band to conduction band, it has to have an energy more than the fermi level.

## Discussion of spectroscopic results

Spectroscopic measurements were carried out at the Sn atomic sites at 77K shows a symmetric trend in both positive and in negative bias. This shows that the valence bands and conduction bands at Sn sites behaves similarly in (100) plane. In this case, more contribution would be coming from the 5p orbitals of Sn atoms. A band gap value of 1 eV was observed from the plot which is comparable to the reported band gap values of SnSe .

Spectroscopic measurements were carried out in the (111) plane of SnSe which showed a different behaviour compared to that of (100) plane. A bandgap value of around 0.25eV was observed in this measurement and this was carried out at 300K. In this case, the bright spots could be either Sn/Se. So the major contributions could be coming from the 5p orbitals of Sn or 4p orbitals of Se. It is possible that what we observe has mixed contributions from the orbitals of Sn and Se.

Spectroscopy was performed at the Sn vacancy defect sites in (100) plane at 77K from -1 V to 1V. The behaviour of this plot was really different from what we observed for the spectroscopy at Sn atoms. In this curve, no electronic states were observed in the negative bias and up to 0.75 V. There is a sudden increase in the electronic states after 0.75 V.

Spectroscopy measurements were performed on 10% bismuth doped SnSe at 300K. Here, bismuth atoms substituted the Sn atoms. A band gap value of more than 1 eV was observed in this system. This could be due to the Burstein Moss effect. As SnSe is doped with electron rich bismuth atoms, more electrons would be added to the system. And bottom of conduction band will be filled with these electrons, further lifting the Fermi level upwards inside the conduction

band . So if the electrons of valence band have to be excited, it has to occupy the bands in the conduction band above Fermi level. So there is an increment of the band gap here.

### 3.13 AFM image and height profile of exfoliated SnSe on gold coated mica

SnSe was exfoliated using an adhesive tape. Once flakes became thinner, it was transferred into PDMS stamp and further to the gold coated mica.

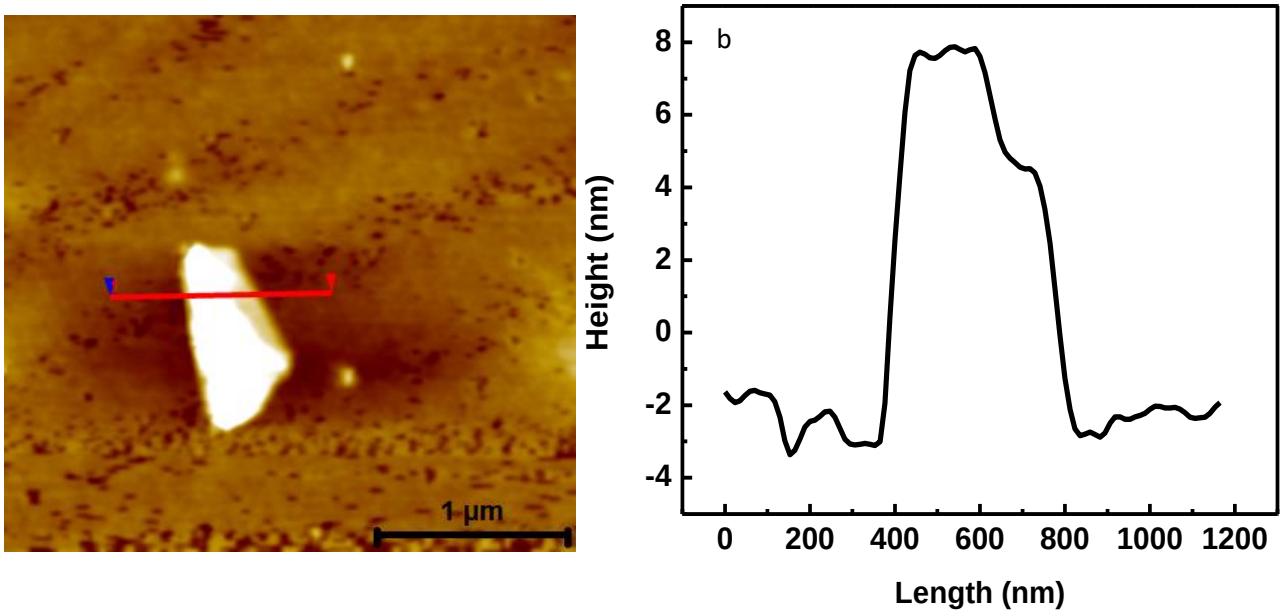


Figure 3.20 (a) shows the AFM image of the exfoliated SnSe and (b) shows its height from the substrate. It could be observed that this flake has 11 and 18 layers of SnSe. Each layer is of 0.6nm height.

This was performed to obtain fewer layers of SnSe. The aim is to do a comparative study of the density of states of few layer( < 10) with that of a bulk

## Conclusions and outlook

In this project, SnSe single crystal was studied using UHV LT STM at 77K. Crystal used was in Pnma phase. Spectroscopic measurements were performed at both 77K and at 300K to reveal the underlying electronic properties of the sample. A bandgap of ~ 1eV was obtained from the STS measurements from UHV LT STM study. Lattice arrangements were studied from atomic resolution images. Hexagonal and rectangular lattices were observed in two different pieces of SnSe single crystal . Lattice parameters of rectangular lattice were found to be b= 4.15 ± 0.03 Å and c = 4.47 ± 0.03 Å and hexagonal lattice shows a lattice parameter of b= 3.98 ± 0.02 Å and c= 3.7 ± 0.01 Å. Two different intrinsic vacancy defects and an intrinsic surface defect of the single crystal were probed in this study. Bi doped SnSe were investigated in room temperature and it showed a variation in the bandgap compared to that of pristine SnSe.

## Future Plans

Spectroscopic studies have to be carried out in various defects to understand how density of states vary there. Bi doped SnSe has to be studied intensively. It would be interesting to observe how the lattice structure accommodates a dopant on Sn site. Comparison of local electron properties of bismuth doped SnSe with pristine SnSe would be interesting.

**Bibliography**

[1] Zhong Lin Wang and Jinhui Song, *Piezoelectric Nanogenerators Based on Zinc Oxide Nanowire Arrays,* SCIENCE VOL **312** (2006)

[2] Ya Yang, Ken C. Pradel, Qingshen Jing, Jyh Ming Wu, Fang Zhang, Yusheng Zhou, Yue Zhang, and Zhong Lin Wang, *Thermoelectric Nanogenerators Based on Single Sb-Doped ZnO Micro/Nanobelts,* ACS NANO, VOL. **6** , 6984–6989 ' (2012)

**[3]** A. K. Geim& I. V. Grigorieva, *Van der Waals heterostructures,* Nature **499**, 419–425 (2013)

[4] A.K. Geim and K.S. Novoselov, *THE RISE OF GRAPHENE*, Nature Materials **6**, 183 - 191 (2007)

[5] Xiaoyan Zhang, Lili Hou, ArturCiesielski, and Paolo Samorì, *2D Materials Beyond Graphene for High-Performance Energy Storage Applications,* Adv. Energy Mater., **6**, 1600671 (2016)

[6]Yuan Liu, Nathan O Weiss, XidongDuan, Hung-Chieh Cheng, Yu Huang, XiangfengDuan, *Van der Waals heterostructures and devices*, Nature Reviews Materials **1**, Article number: 16042 (2016)

[7]Introduction to Thermoelectricity. Authors: Goldsmid, H. Julian

[8]M. Gharsallah, F. Serrano-Sánchez, N. M. Nemes, F. J. Mompeán, J. L. Martínez,M. T. Fernández-Díaz, F. Elhalouani, J. A. Alonso, *Giant Seebeck effect in Ge-doped SnSe*, Scientific Reports**6**, 26774 (2016)

[9]A. Gyenis, I. K. Drozdov, S. Nadj-Perge, O. B. Jeong, J. Seo, I. Pletikosi´c T. Valla, G. D. Gu, and A. Yazdani, *Quasiparticle interference on the surface of the topological crystalline insulator* $Pb_{1-x}Sn_xSe$,PHYSICAL REVIEW B **88**, 125414 (2013)

[10] Arpan Krishna Deb and Vijay Kumar, *Bandgap engineering in semiconducting one to few layers of SnS and SnSe,* Phys. Status Solidi B, **1–8** (2016)

[11] KritiTyagi, BhaskerGahtori, SivaiahBathula, Niraj Kumar Singh, Swati Bishnoi S. Auluck, A. K. Srivastava and Ajay Dhar, *Electrical transport and mechanical properties of* thermoelectric tin selenide ,RSC Adv., **6**, 11562 (2016)

[12] Xuliang Chen, Xuefei Wang, Yonghui Zhou, Chao An, Ying Zhou, Cong Xian, BinyangHou, Changyong Park, Kunling Peng, Xiaoyuan Zhou, YiminXiong , Zhaorong Yang , and Yuheng Zhang ,*Rocksalt phase and superconductivity in pressurized SnSe* arXiv:**1608**.06763v2 ,(2016)

[13]C. W. Li1, J. Hong1 , A. F. May , D. Bansal , S. Chi , T. Hong , G. Ehlers and O. Delaire,*Orbitally driven giant phonon anharmonicity in SnSe,* Nature Physics**11**, 1063–1069 (2015)

[14] Li-Dong Zhao , Shih-Han Lo , Yongsheng Zhang , Hui Sun , Gangjian Tan , CtiradUher , C. Wolverton , Vinayak P. Dravid&Mercouri G. Kanatzidis, *Ultralow thermal conductivity and high thermoelectric figure of merit in SnSe crystals*, Nature **508**,373–377 (2014)

[15]XueWang, JingtaoXu, GuoqiangLiu, YajieFu, Zhu Liu, XiaojianTan, HezhuShao, HaochuanJiang, TianyaTan,and Jun Jiang, *Optimization of thermoelectric properties in n-type SnSe doped with BiCl3,*APPLIED PHYSICS LETTERS **108**, 083902 (2016)

[16]Anh Tuan Duong, Van Quang Nguyen, GanbatDuvjir, Van Thiet Duong, Suyong Kwon, Jae Yong Song, Jae Ki Lee, Ji Eun Lee, SuDong Park, Taewon Min, Jaekwang Lee, Jungdae Kim &Sunglae Cho, *Achieving ZT = 2.2 with Bi-doped n-type SnSe single crystals*, Nature Communication **13713** (2016)

[17]J.C. Li , D. Li , X.Y. Qin, J. Zhang. *Enhanced thermoelectric performance of p-type SnSe doped with Zn,*ScriptaMaterialia**126** (2017) 6–10

[18] Eyob K. Chere, Qian Zhang, KeshabDahal, Feng Cao, Jun Mao and ZhifengRen,*Studies on thermoelectric figure of merit of Na doped p-type polycrystalline SnSe,* J. Mater. Chem. A, **4**, 1848

[19] Cheng-Lung Chen, HengWanga Yang-Yuan Chen, Tristan Day and G. Jeffrey Snyder, *Thermoelectric properties of p-type polycrystalline SnSe doped with Ag,* J. Mater. Chem. A, **2**,1117,(2014)

[20] Sang-ui Kim, Anh-Tuan Duong, Sunglae Cho, S.H. Rhim , Jungdae Kim, *A microscopic study investigating the structure of SnSe surfaces,* Surface Science **651** 5–9 (2016)

[21] Paolo Sessi, Domenico Di Sante, Andrzej Szczerbakow, Florian Glott, Stefan Wilfert, Henrik Schmidt, Thomas Bathon, Piotr Dziawa, Martin Greiter, Titus Neupert, Giorgio Sangiovanni, Tomasz Story, Ronny Thomale, Matthias Bode1 , *Robust spin-polarized midgapstates at step edges of topological crystalline insulators,* Science TOPOLOGICAL MATTERS, VOL **354** ISSUE 6317 (2016)

[22]Zhenyu Wang , Jianfeng Wang , YunyiZang , Qinghua Zhang , Jin-An Shi , Tian Jiang , Yan Gong , Can-Li Song , Shuai-Hua Ji , Li-Li Wang , Lin Gu , Ke He ,WenhuiDuan , Xucun Ma , Xi Chen , and Qi-Kun Xue , *Molecular Beam Epitaxy-Grown SnSe in the Rock-Salt Structure: An Artificial Topological Crystalline InsulatorMaterial,*Adv. Mater., **27**, 4150–4154 (2015)

[23] Introduction to Scanning Tunneling Microscopy, C. Julian Chen

[24] Aparna Deshpande, Brian J. LeRoy, *Scanning probe microscopy of graphene* , Physica E **44** 743–759 (2012)

[25] MODERN Vacuum PRACTICE, NIGEL HARRIS

[26] BIN XU, JING ZHANG, GONGQI YU, SHANSHAN MA,YUSHENG WANG, and LIN YI, *Comparative Study of Electronic Structure and Thermoelectric Properties of SnSe for Pnma and Cmcm Phase,* Journal of ELECTRONIC MATERIALS, (2016)